Available online at www.CivileJournal.org

Civil Engineering Journal

Vol. 5, No. 2, February, 2019

Behavior of Laminated Reinforced Concrete Curved Beam with Changing Concrete Properties

Hesham A. Numan [a*], Waleed A. Waryosh [a], Shaima Sabri Ali [a]

[a] *Civil Engineering Department, Faculty of Engineering, Al-Mustansiriayah University, Baghdad 10052, Iraq.*

Received 11 December 2018; Accepted 07 February 2019

Abstract

Strengthening and upgrading the performance reinforced concrete curved structures for functional purpose as well as for conversation of architectural aesthetic aspect is the main concern for engineers. In the present study, four full-scale experimental Curved Reinforced Concrete (CRC) beams conducted. The cross-section of all CRC beams was T-section. The parametric studies are carried out to investigate the effect of time of casting segmental layers (web and flange) and the compressive strength of concrete on the structural behavior of such structures. Three values of compressive strength of concrete used in this study, these are (25, 50, 75 MPa). The control specimen casting as one unit with the compressive strength of concrete was 25 MPa. The present outcomes showed that the increase in the compressive strength of concrete up to 75 MPa of the flange zone plays a significant role in raising the ultimate capacity by 22.86% and reducing the deflection by 61.43% in the quarter span as compared with control specimen. Additionally, the trend and distribution of cracks, mode of failure, and strain response of CRC specimens are briefly discussed in this study.

Keywords: Curved Reinforced Concrete; Compressive Strength; Time of Casting; Laminated Structure.

1. Introduction

The major feature of the CRC structure is that, if the curve is fittingly shaped, the whole cross-section can be used in compression under the extreme (complete) load [1]. As CRC structure has been an engineering and scientific topic for more than three centuries; many methods such as graphical methods have been presented to analyze this kind of structure [2].

Several analyzes suggested by (Khalifa [3]; McMullen et al. [4]; Hsu et al. [5]; Mansur and Rangan [6]; Franciosi [7]) to study the collapse for certain cases of CRC beams. By using the finite element method, Zhenfei and Dawen [8] analyzed the indeterminate CRC. The outcomes of this study referred that the actual performance of the CRC was nonlinear. The hinged circular arch investigated by Yang and Shieh [9] through dividing the arch to twenty-five straight elements with equal length with assuming two load cases. Under the effects of live load, a full span of reinforced arch culvert bridge modeled and analyzed by McGrath and Mastroianni [10]. The main conclusion of this study that the two-dimensional models have limited ability to foretell the longitudinal spreading of live load forces in the culverts. A nonlinear three-dimensional finite element simulation carried out by Husain et al. [11] to analyze the effect of the curvature (L/R ratio of 0, 0.1, 0.15 and 0.2) on the demeanor of the curved in plan composite concrete beams. Kang and Tan [12] used the energy balance hypothesis to estimate the compressive arch action of reinforced concrete beam-column subassemblages. Falamarz-Sheikhabadi et al. [13] conducted an analysis study on the tall long-span curved reinforced-concrete under time history response to uniform and spatially variable seismic excitations, nonlinear static pushover, and incremental dynamic methodology to assess the structural performance for such construction.

* Corresponding author: dr.heshamnuman@uomustansiriyah.edu.iq

http://dx.doi.org/10.28991/cej-2019-03091244

Furthermore, based on the study conducted by Anas [14] to assess the demeanor of CRC in-plane beams, the author found that the difference between numerical and available experimental results in the ultimate load within the range 4-8%. The influence of utilizing composite un-bonded tendons to the extrados surface of a semi-circle arch as another alternative for arch strengthening was studied analytically by D'Ambrisi et al. [15]. The numerical analysis carried out by Qi et al. [16] to determine the dynamical response of CRC exposed to blast loading, the results indicated that the zone near the explosion has large local deformations with great damaged. Based on a theoretical study, Abbasnia and Nav [17] presented the procedure to estimate the structural robustness and also the arching capacity of beams. Additionally, through activating three-dimensional finite element approach of an actual existing deck-type reinforced concrete arch bridge, Farahani and Maalek [18] referred that the influences of the vertical component of ground motion must be included in the analysis of such construction.

The strengthening design of the CRC bridge that reached to the end of life service using a carbon fiber reinforced polymer conducted by Li et al. [19] was very convincing under the static and dynamic loadings. Nam et al. [20] suggested a design procedure for CRC section strengthening by fiber reinforced polymer that exposed to blast loading. The authors founded that the existence of fiber reinforced polymer worked to increase the resistance of the arch section under the blast loading. Moreover, Hesham [21] studied the effect of increasing compressive strength of concrete (22, 45 and 71 MPa) on the structural beam behavior. He used the super-plasticizer and Glenium 51 as additives material to the concrete to increase the compressive strength. Gou et al. [22] determined the local stress distributions of the V-shape pier-girder joint under different loading conditions. Additionally, according to the study accomplished by Gou et al. [23] on the Yichang Yangtze River Bridge to investigate the stress distributions in the girder-arch-pier connections. A testing loading scheme depends on the Italian Code adopted by Martinelli et al. [24] to investigate the bearing capacity of arch bridge in Lecco (northern Italy). Under quasi-static and cyclic loading systems, Augusthus-Nelson [25] investigated the demeanor of soil-filled masonry arch bridges.

Based on the study accomplished by Hoehler et al. [26] on the concrete arch bridge in California demonstrated that the accurate modeling of expansion joints in particular; was critical to achieve representative the modal and transient demeanor. Marefat et al. [27] indicated that the arch concrete strong and stiff against the static and dynamic loads, but the cracks can be developed and created when the applied loads greater than service load. The first cracks, main reinforcement corrosion, and variation of the arch axial line shape were important effected on the ultimate strength and failure mode of the CRC bridge based on the investigation carried out by Zhang et al. [28]. The ultimate capacity of the arch concrete section varies nonlinearly with the initial geometric imperfection. Besides the relationship between the ultimate capacity and the length to the radius ratio of the arch rib is a cube curve. These considerations depend on study conducted by Song et al. [29]. Tamura and Murata [30] determined the main factors that affected the behavior of CRC, which were the radius of curvature and axial force.

The fixed-ends of CRC beams with a non-uniform distribution of longitudinal reinforcements worked to improve the ultimate load capacity of 23.5% based on the study conducted by Al-Mutairee [31]. The previous researchers (Bharadwaj and Purushotham [32]; Muralidharan et al. [33]) confirmed that some parameters such as compressive strength of concrete, depth of the beam, support conditions, radius of curvature, span ratio, and tensile strength of steel play a major role in the behavior of CRC. With various end constraints, Lee and Jeong [34] studied the natural frequencies and mode shapes of curved beams. Li et al. [35] presented the key procedure and constructional details of the negative angle vertical rotating construction method on the CRC bridge constructed in China that was Pearl Bridge.

Three main configurations of concrete arch bridges; these are light deck arch, deck arch, and half-through arch [36]. Previous studies reported on the seismic guidelines of analysis and design of real deck arch bridges such as (Kawashima and Mizoguchi [37]; Žderić et al. [38]; Šavor et al. [39]; Franetović et al. [40]). Furthermore, Khan et al. [41] extended the direct displacement-based design method that spliced for buildings and bridges to arch design. They suggested a new approach of arch design applied to three case study deck arch bridges in cases of longitudinal and transverse directions, besides the designs were validated by nonlinear time-history analyses.

The load-bearing capacity and ductility for stone arches raised by using a basalt textile embedded in an organic matrix according to a study presented by Garmendia et al. [42]. The behavior of reinforced concrete and masonry arch bridge under the effect of seismic loading discussed by Modena et al. [43]. Static and seismic retrofitting illustrated, and so many problems involved taking into account several load cases. The main parameters were selected based on the maintain methodology of the arch bridge, repair methods and strengthening system. Concluded that based on the behavior of retrofitting that there are enhanced in the strength capacity of the arch bridge. The masonry arches wall strengthened by a different configuration of sandwich Carbon-fiber Reinforced Polymer conducted by Anwar [44] to evaluate the strength efficiency and the full behavior of the wall. It found that the effectiveness of strengthening of quarter circle arch less than that of the semi-circle arch for the same strengthening configuration. Additionally, Valerio et al. [45] used a polybenzoxazole fabric reinforced cementitious mortar composite to improve the mechanical performance of masonry arches.

The above literature survey, besides the extensive research in the articles published about this field of study accomplished by the authors, it has been confirmed that the experimental investigation of CRC beams is really rare. Hence, to fill this gap in the scientific research on the knowledge real structural behavior of such construction; four full-

scale CRC beams with abutments conducted and tested experimentally. On the other hand, the influences of different time of casting segments (web and flange zone) and the change of the compressive strength of concrete on the full performance of such structures studied.

2. Materials and Methods

The equipment and instruments belong to the construction and structural laboratories of the civil engineering department /Al-Mustansiriayah University employed to achieve the experimental program in this study. The following sections illustrated the material used, mechanical properties, specimens, and test procedure in the current study:

2.1. Material Used

The components of concrete were: the type of cement was Ordinary Portland Cement (OPC-Type 1), the size of coarse aggregate was 10 mm, and fine aggregate with a maximum size was 4.75 mm utilized in all casting of specimens. Figure 1 illustrated the sieve analysis results of coarse and fine aggregate used. From this figure, it clearly can be seen the results of sieve analysis of the use aggregates were within the range (lower and upper limits) that specified by Iraqi Specification No.45/1984 [46]. Silica fume was adopted as the brand of commercially known as partial add to cement because of play an effective in improving the mechanical properties of concrete. Besides the GLENIUM51 was used as a super-plasticizer material to the concrete mixture. The tap water used for mixing and curing the concrete specimens without water treatment. On the other hand, the diameter of steel reinforcement used was 10 mm, and 12mm.

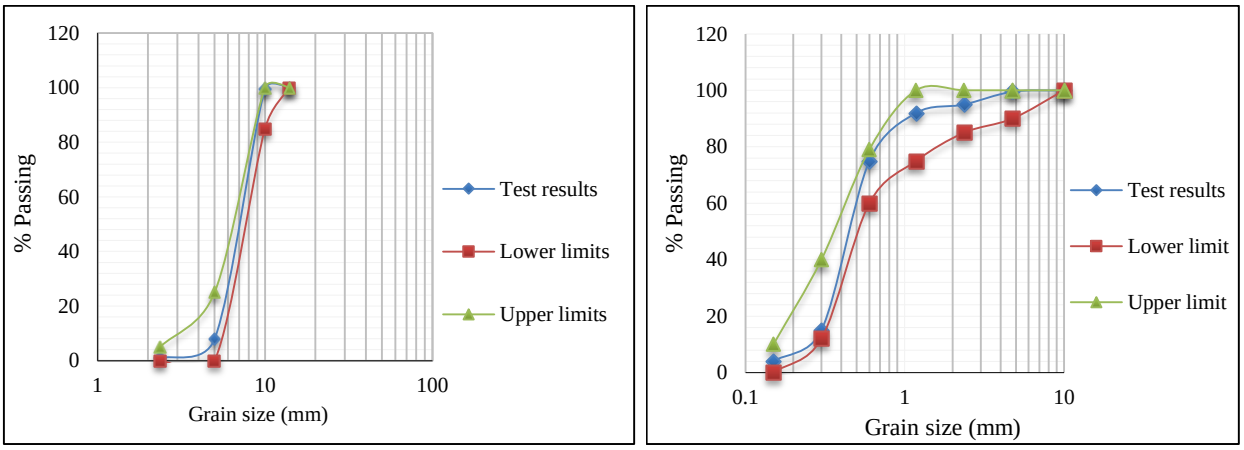

a) **b)**

Figure 1. Sieve analysis of : (a) Coarse aggregate, (b) Fine aggregate

2.2. Mechanical Properties

In this study, the mix design of concrete was (1:1.5:3) by weight with a water-cement ratio (0.45). Normal and high compressive strengths of concrete (fc') achieved, these are 25, 50, 75 MPa. After each mixing trail of the concrete, the mean value of three standard concrete cylinders (300 mm height and 150 mm diameter) under the compressive strength test taken into account to achieve the accuracy for obtaining the required value of compressive strength of the concrete mixture. The compressive strength of concrete measured based on the recommendations of ASTM C39-01 [47]. Based on tensile tests conducted, the properties of steel reinforcement (10 and 12 mm) used in the current study listed in Table 1.

Table 1. Properties of steel reinforcement used

Nominal diameter (mm)	Measured Diameter (mm)	Yield tensile strength f_y (MPa)	Ultimate tensile strength f_u (MPa)	E_s (GPa)
10	9.92	405	596	200
12	12.41	410	610	200

2.3. Details of Test Specimens

Figure 2 illustrates the configuration and dimensions of the full-scale CRC beams with the abutments. The cross-section at the mid-span for each specimen was T-section. The height of all the specimens from the intrados surface and the extrados surface of the specimen to the ground surface was 500 and 875 mm, respectively. The rest dimensions of the specimens clearly illustrated in Figure 2. The main reinforcement at both the top and bottom face were (3ϕ12), while the stirrups with the diameter (ϕ10) at 150 mm center to center. The boundary conditions of specimens were simply supported.

Four specimens are taken into account in this study to emulate the effects of time of casting and type of concrete on the action for such structural elements. The first one (SP1), the web and flange zone casting together as one unit with the same compressive strength (25 MPa) and considered as the control specimen. The other three specimens (SP2, SP3, SP3), after completing full-range of seven days from casting of the web zone, then casting the flange zone. Besides these specimens has the same compressive strength at the web zone and was 25 MPa, while it varied at flange zone, which was 25, 50, 75 MPa, respectively. However, Table 2 shows the description of casting case and compressive strength of concrete for two-segment parts (web and flange) of each specimen. SP abbreviate to the specimen, while (1, 2, 3 and 4) indicate to the number of specimens.

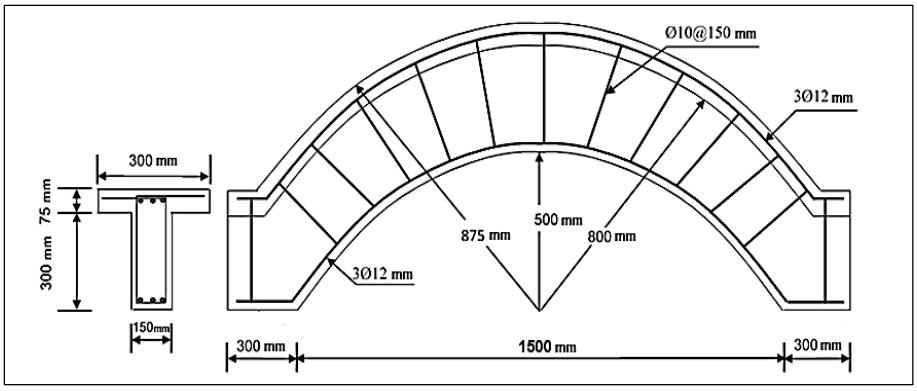

Figure 2. Configuration and geometry of CRC beam with abutments

Table 2. Specimens details

Model mark	Description of casting	Compressive strength of flange zone (f_c') (MPa)	Compressive strength of web zone (f_c') (MPa)
SP1*	As one unit	25	25
SP2	Laminated	25	25
SP3	Laminated	50	25
SP4	Laminated	75	25

*Control specimen

2.4. Test Procedures

The specimens exposed to the static load (one point load) at the top face of the middle span and distributed across the entire width of the beams by using a solid rod, as shown in Figure 3. The load applied progressively with smaller increments of 5 kN until approaching the failure load (90% of the load capacity of specimens). For each time step of loading, deflections and strains in concrete and steel reinforcement measured. Each specimen painted with white color to diagnose any crack formation during the tests. The tests are carried out by using a Universal Testing Machine (UTM) brand as (8551 M. F. L. System) with a capacity of (3000 kN), as depicted in Figure 3. To ensure from removing the effect of friction and undesirable bearing stress concentrations, soft wooden boards placed between the steel tubes and the base of the test frame. The data acquisition system mainly consists of multiplexer type B-2760, and TC-32K handheld data logger. On the other hand, the sensors used were: two dial indicators (Mitutoyo-2046S) with a minimum reading of 1/100 mm), and four TML strain gauges (two surfaces for concrete and two embedment strain gauges for steel rebar). The dimensions of surface strain gauges used were (5 × 1 cm), while the dimensions of embedment strain gauges used were (6 × 2 mm).

Figure 3. The specimen in the UTM

3. Results of Testing

3.1. Deflection and Cracks

At all stages of loading up to failure, the vertical displacement registered at two sites that are at the intrados surface in quarter and mid-span of each CRC specimen. The reason for selecting these sites specific to more conception on the trend and the demeanor of the deflection values of the critical region of this structure at each time-step of loading. Figure 4a and 4b illustrates the full behavior of loads-deflections at a quarter and mid-span for four CRC specimens, respectively.

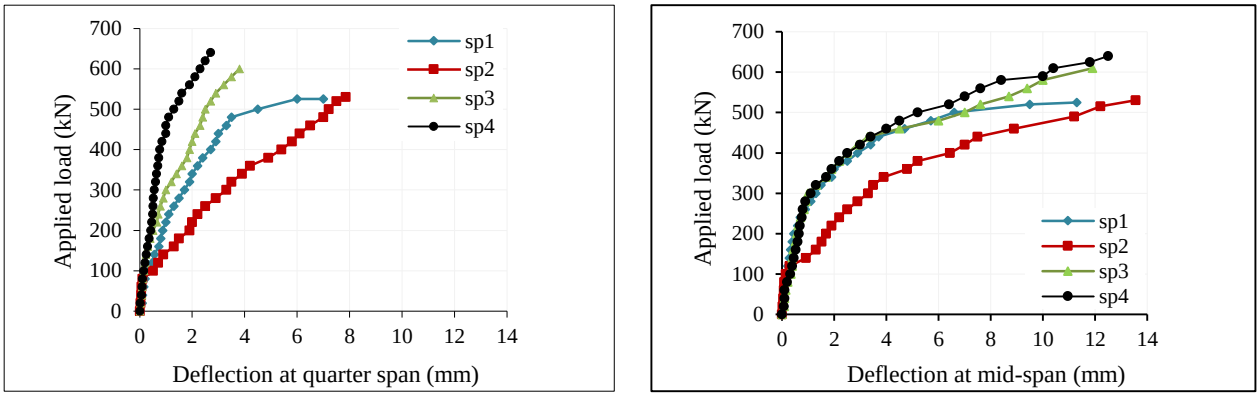

a) **b)**

Figure 4. (a) Load against deflection behaviors at a quarter span of the specimens, (b) Load against deflections behaviors at a mid-span of the specimens

From Figure 4, it clearly noticed that the behavior of all tested specimens started as linear up to the inflection point that represents the first crack, and then the curve became nonlinear. The reason for the nonlinearity behavior of load-deflection after occurring the first crack due to the decrease in beam stiffness as a result of reducing the modulus elasticity of concrete under increasing the magnitude of the applied load. The inflection point as the percentage of the ultimate load capacity developed based on the tension resistance of the specimen. Table 3 summarized the loads at the first crack and ultimate, besides the deflection in the quarter and mid-span of the CRC with corresponding to the first crack and ultimate loads. However, a general observation on the results in Figure 4 that the stiffness of specimens reduced according to the increment of the applied load until approaching to failure.

Table 3. Load and deflection results summarized for all specimens

Specimen mark	First cracking load P_c (kN)	Ultimate load P_u (kN)	Deflection at first cracks (mm)		Deflection at ultimate load (mm)	
			Quarter span	Mid-span	Quarter span	Mid-span
SP1	105	525	0.45	0.53	7.00	11.10
SP2	108	530	0.65	0.70	7.85	13.55
SP3	185	600	0.21	0.45	3.86	11.75
SP4	201	645	0.17	0.35	2.7	12.63

Other main notes about the trend of the relationship between the increment load and the recorded deflections at the quarter and mid-span of all specimens briefly discussed in the following paragraph:

In the case of SP1, the relationship was linearity up to 20% from the ultimate load, which represents the percentage ratio between the load caused to appear the first crack to the load capacity of the specimen. At the failure load, the maximum deflection recorded in the mid-span of the specimen and was 11.10 mm. The reason for registering peak value of deflection in the mid-span of the specimen due to the cumulative deflection slip from support and concentrated at the point under the load application. The same reason explained to us why the peak value of deflection recorder at the mid-span for the other three specimens at the failure load. On the other hand, the maximum value of deflection decreased by approximately 37% when approached in the quarter position in the ultimate load stage.

A slight increase in the ultimate load in SP2 as compared with the control specimen and was 0.95%. Besides that increase of the load of appearance the first crack did not exceed 2.86% as compared with SP1, this means the trivial increment almost never remembered in the linear behavior capacity of this specimen occurred when compared with the control specimen. In general, the results in Figure 4 demonstrated that the increase in deflection values in SP2 was larger than the control specimen under the same load applied. On the other hand, the maximum deflection value also registered at the mid-span of this specimen in the failure load which was 13.55 mm with an increase of 22.07% of the maximum deflection recorded in SP1. This is because the slip generated at the interface zone between the web and flange layer

result from the interaction between these layers was partial. The amount of decreasing in the peak deflection of the SP2 was about 42.07% when transferred from middle to quarter span of the specimen at the failure load. However, in spite of little increase of the ultimate load capacity in SP2 with compared to the control specimen; but the highest percentage increase of deflections in the failure load recorded of SP2 than others. This goes back to the casting process has done as layers in SP2 with a lower compressive strength of concrete (25 MPa).

The ultimate load in SP3 increased by 14.29% as compared with the control specimen. Moreover, the SP3 behaved as a linear relationship up to 31% from the load that appears the first crack to the ultimate load. This means that the extent in the linear behavior of SP3 as compared by the SP1. These results due to the compressive strength of the flange that resists the moment increased, and hence the increase in internal resistance of the SP3 took place. At the failure load, the peak deflection recorded in the mid-span of SP3 and was 11.75 mm. This value decreased by 67.15% when transferring from middle to quarter region of SP3.

Even the casting the flange zone after seven days from casting web zone, but increasing in compressive strength (75 MPa) in the flange zone of SP4 worked to increase in stiffness due to increase in the modulus of elasticity, and hence, increasing in the strength capacity of this specimen as compared to control specimen. Therefore, the peak value of ultimate load recorded at SP4 and was 645 kN with increasing of 22.86% of what happened in the control specimen. For the same reason, it found the maximum percentage of reduction in the deflection in the quarter span in the failure load recorded between SP4 and the control specimen and was 61.43%. However, the maximum deflection of SP4 took place in the mid-span and was 12.63 mm which decreased by 78.62% when transferring from middle to quarter span at the final stage of loading. The increment in the ultimate load capacity of SP3, and SP4 caused to increase the mid-span deflections at the final stage of loading as compared with the control specimen. The linearity behavior in SP4 and SP3 was pretty much convergent. This goes back to the percentage ratio of the appearance of the first crack to the ultimate load in these specimens was very close.

Another important notice on the results in Table 3 that when increasing the compressive strength of concrete (50 and 75 MPa) in SP3 and SP4; the first crack delayed from the appearance as compared with the control specimen. This is due to the increase in the tensile strength and modulus of rupture in these specimens.

Figure 5 illustrates the mode of failure and the developed cracks due to increased loads up to failure for all specimens. In general, the cracks appeared in the tension zone at the early stages of loading and with the progressing of loading stage; these cracks increased in number, became wider, and directed to upwards at the center of the applied load. At about 70% of the load capacity for all specimens, the main cracks developed in the tension zone and often combined with each other. These cracks propagated and continued upward until approaching to the upper face of the specimen, where crushing of concrete took place. Due to increase the modulus of elasticity when increased the compressive strength of concrete (50 and 75 MPa), the main cracks reduced as clearly depicted in Figure 5.

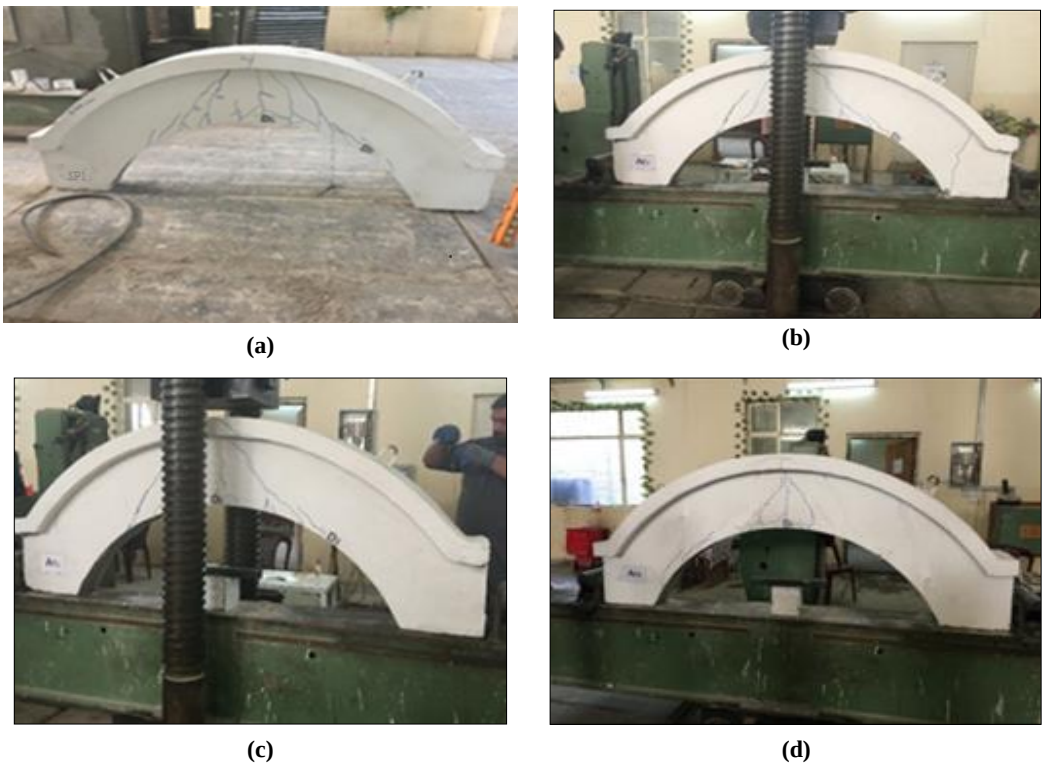

(a) **(b)**

(c) **(d)**

Figure 5. The developed cracks after the tests (a) SP1, (b) SP2, (c) SP3 and (d) SP4

3.2. Strain Response

In all CRC beams, two strain gages distributed at the positions 2 and 3 to measure the strain behavior of the concrete, while two strain gages distributed at the positions 1 and 4 to examine the strain behavior of steel reinforcement. Figure 6 shows the strain gages distribution in CRC beams.

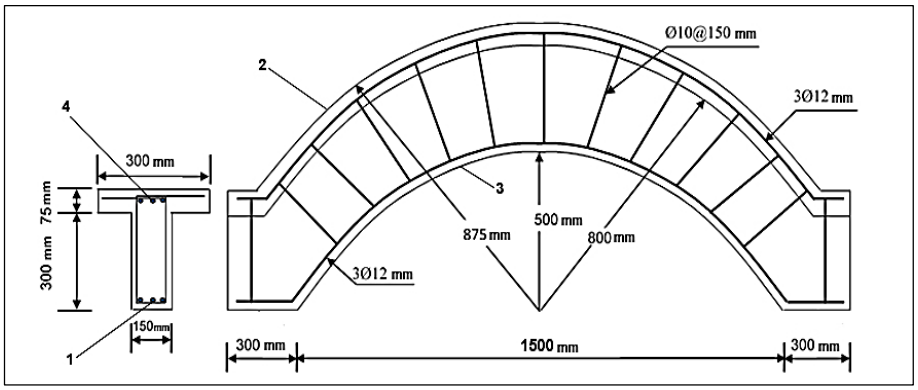

Figure 6. Strain gages layout

The reason for selection position 2 and 3 in the concrete region to represent the strain behavior at the compression and tension zone, respectively. Based on the ACI-318-14 [47] the strain in the normal concrete not greater than 0.003 in the compression zone and it becomes smaller in the tension zone. Results in Figure 7 illustrate the peak values of strain achieved in position 2 (compression zone), and they became smaller in position 3 (tension zone). The peak value of strain registered in the compression zone of concrete and was 0.0021, 0.0027, 0.0036 and 0.0047 with SP1, SP2, SP3 and SP4, respectively as shown in Figure 7a. The reason of the peak strains in SP2, SP3 and SP4 were close or exceeded to the limit of strain (0.003) that recommended by ACI-318-14 [48] due to generation slip strain result from built these specimens as the laminated system. However, the maximum percentage difference of the peak strain in concrete occurred between SP4 and SP1 and was 76.47%. This goes back the process of transferring load was very slow from flange segment to the web segment in SP4 than others result from approaching to the peak compressive strength of concrete (75 MPa) in the flange segment.

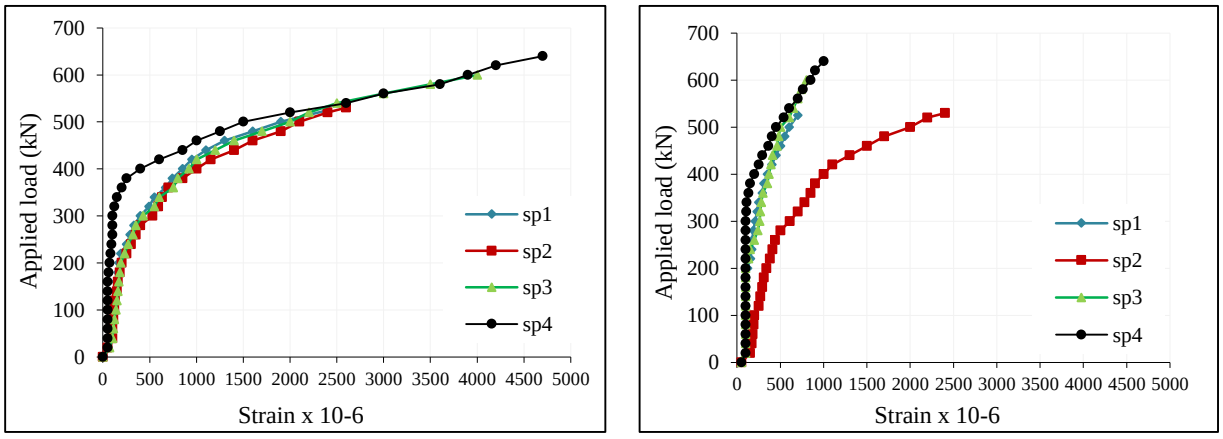

a) **b)**

Figure 7. Strain in the concrete (a) at the position 2, and (b) at the position 3

The strains in the reinforcements up to the yield strength that represents the inflection point to the elastic-plastic behavior. The strains of main reinforcements measured at the location (1 and 4), which chosen specifically to examine the strain at tension and compression zone. The results of strain in tension and compression zones of main steel reinforcement illustrate in Figure 8 (a and b). From this figure, in general, it found the trend of strain curves in all specimens at two positions was similar to a large extent. Another important note in this figure that is the minimum value of strain in the steel reinforcement registered at position 4 in SP4 (0.0015) due to increase the compressive strength (75MPa) enhanced in the tensile strength of concrete at the flange zone, as depicted in Figure 8 (b). On the other hand, the maximum value of steel reinforcement recorded at SP3 in position 1 (0.0042) and a small difference detected with the maximum value of SP4 at the same position, as illustrated in Figure 8 (a), where the percentage difference between them did not exceed 10%. The registered maximum value of strain rebar in position 1is considered logically due to this position represents the tension zone of the system.

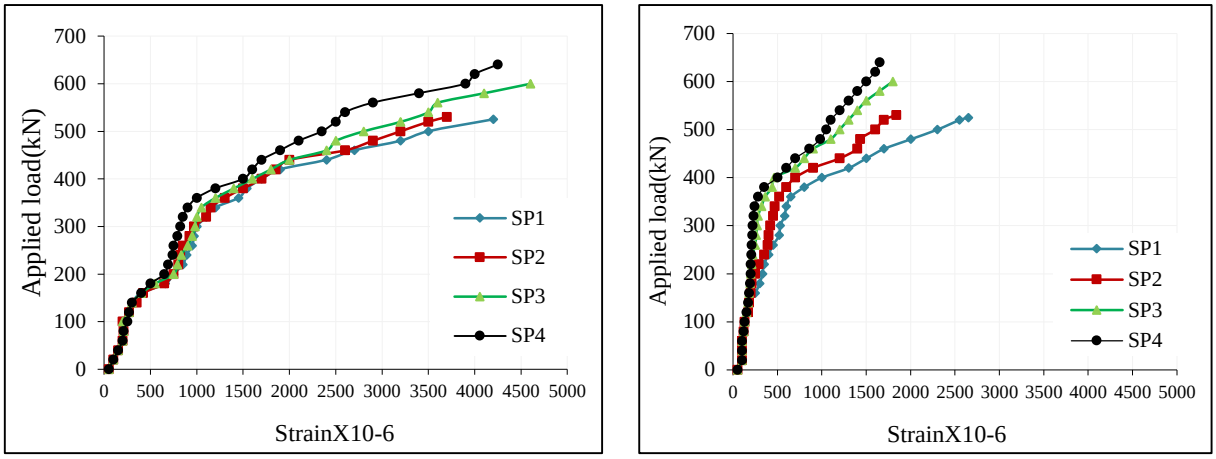

Figure 8. Strain in the main reinforcement (a) at the position 1 and (b) at the position 4

4. Conclusion

Due to a curved beam resists gravity loads in compression, the CRC beam can be seen as an effective and elegant means of benefitting from the rise compression resistance of concrete. For more visualization about the structural action of T-section CRC beams under static loading; four experimental full-scale CRC specimens with abutments conducted. The influences of casting web and flange zone as laminated layers with a different time, besides the changing of concrete properties in the flange zone on full performance for such structural elements studied. Based on the outcomes of this study, the main conclusions summarized in the following points:

- The increase in the compressive strength of concrete at the flange zone from 25 to 75 MPa with variation step 25 MPa of CRC specimens worked to raise the load capacity by 14.29% and 22.86% in SP3 and SP4, respectively as compared to the control specimen. Additionally, the increasing the compressive strength of concrete at the flange zone resulted in the delay from the appearance the first crack with an increase in the load was 76.19% and 91.43% in SP3 and SP4, respectively as compared with control specimen. From these findings, it concluded that the value of compressive strength of concrete in the flange segment was a major effect on both of ultimate load capacity and the trend of CRC specimens without any influence of casting the flange part and web part at a different time. The influence of different casting time was limited when compared between SP1 and SP2 (with the same compressive strength) that is in SP2 somewhat delay of the appearance first crack and an insignificant increase in the ultimate load as compared with SP1.
- The flexural cracks appeared at the bottom face of all CRC specimens, which started from the tension zone within the range of 20% to 30% from the ultimate load capacity of the beams, and then increased in number and become wider with the progress of applying load. Then, these cracks propagated and continued upward until approaching to the upper face of the specimen at the final stages of loading, where crushing of concrete took place. When increasing the compressive strengths (50 and 75 MPa) in SP3 and SP4 led to reduce the formation of main cracks as compared to the control specimen.
- The peak strain of concrete recorded at the compression zone in SP4 and was 0.0047. This value decreased by 55.32%, 42.55% and 23.40% when transferring from SP4 to control specimen, SP2, and SP3, respectively. The peak value of concrete strains for SP3 and SP4 exceeded the limit of strain that recommended by the ACI-318-14, with a percentage difference ranged from 18.18% to 44.15% result from the laminated system in these specimens. However, the minimum percentage difference of the peak strain in concrete took place between SP2 and control specimen and was 25%, while the maximum percentage difference of the peak strain in concrete happened between SP4 and control specimen and was 76.47%.
- For the selection position in the steel reinforcement, the trend of the distribution of the strain in steel reinforcement versus the applied load for all CRC specimens was similar by and large. The minimum value of strain in the steel reinforcement registered in the compression region in SP4 (0.0015). On the other hand, the maximum value of steel reinforcement recorded at SP3 in the tension region and was 0.0042 with somewhat small differences detected for the recorded maximum value of steel reinforcement strains for the rest specimen at the same position.

5. Funding

Al-Mustansiryah University allowed the use of it laboratories for authors in this research, but the authors have no support or funding from Al-Mustansiryah University, agency, and other sectors. The authors certify that they have non-

financial interest (such as personal or professional relationships, affiliations, knowledge or beliefs) in the subject matter or materials discussed in this manuscript.

6. Conflicts of Interest

The authors declare no conflict of interest.

7. References

[1] Edward, S. H., and David P. G. "Building Design and Construction Handbook" (2004). Section Nine-Concrete Construction, McGraw-Hill, New York, USA.

[2] Kim, J.S., Garro, R., and Doty, D. "A Simplified Load Rating Method for Masonry and Reinforced Concrete Arch Bridges." Proceeding conference of the American Railway Engineering and Maintenance-of-Way Association (September 2009): 1-37.

[3] Khalifa, Magdi Mohamed Ahmed. "Collapse of reinforced concrete beams curved in plan." Master's thesis, Calgary, 1972. doi:10.11575/PRISM/15252.

[4] Badawy, H. E. I., A. E. McMullen, and I. J. Jordaan. "Experimental Investigation of the Collapse of Renforced Concrete Curved Beams." Magazine of Concrete Research 29, no. 99 (June 1977): 59–69. doi:10.1680/macr.1977.29.99.59.

[5] Hsu, T.T., Inan, M., and Fonticiella, L. "Behavior of Reinforced Concrete Horizontally Curved Beams." American Concrete Institute Journal 75 (April 1978): 112-123.

[6] Mansur, M. A., and B. V. Rangan. "Collapse Loads of Nonprestressed R/C Curved Beams." Journal of Structural Engineering 109, no. 4 (April 1983): 993–1009. doi:10.1061/(asce)0733-9445(1983)109:4(993).

[7] Franciosi, C. "A Simplified Method for the Analysis of Incremental Collapse of Reinforced Concrete Arches." International Journal of Mechanical Sciences 26 (December 1984) : 445-457. doi: 10.1016/0020-7403(84)90034-1.

[8] Zhenfei Z. and Dawen P. "NonLinear Analysis of Statically Indeterminate Reinforced Concrete Arches [J] ". Journal of Fuzhou University (Natural Sciences Edition) 02 (1985): 116-127. doi: 10.11908/j.issn.0253-374x. 2018.11.00.

[9] Yang, Y.B., and Shieh, M.S. "Solution Method for Nonlinear Problems with Multiple Critical Points. " The American Institute of Aeronautics and Astronautics Journal 28 (January1990): 2110-2116. doi:org/10.2514/3.10529.

[10] McGrath, T. J., and Mastroianni, E. P. "Finite-Element Modeling of Reinforced Concrete Arch under Live Load Arch under Live Load. " Transportation Research Board 1814 (January 2002): 203-210. doi: 10.3141/1814-24.

[11] Husain, H.M. , Hamood, M.J., and Shaima'a T. S. "Analysis up to Failure of Straight and Horizontally Curved Composite Precast Beam and Cast-In-Place Slab with Partial Interaction. " Engineering and Technology Journal 27 (April 2009): 2509-2522.

[12] Kang, S.B., and Tan, K.H. "Analytical Model for Compressive Arch Action in Horizontally Restrained Beam-Column Subassemblages. " Journal American Concrete Institute Structural (July-August 2016), Technical Paper no. 113-S70: 813-826. doi: 10.14359/51688629.

[13] Falamarz-Sheikhabadi, M.R., and Zerva, A. "Analytical Seismic Assessment of a Tall Long-Span Curved Reinforced-Concrete Bridge. Part I: Numerical Modeling and Input Excitation." Journal of Earthquake Engineering 21(2017):1305-1334. doi:10.1080/13632469.2016.1211565.

[14] Anas, H. Y. "Evaluation of the Behaviour of Reinforced Concrete Curved in-Plane Beams." Iraqi Journal of Civil Engineering 6 (January 2010): 14-25.

[15] D'Ambrisi, Angelo, Luciano Feo, and Francesco Focacci. "Masonry Arches Strengthened with Composite Unbonded Tendons." Composite Structures 98 (April 2013): 323–329. doi:10.1016/j.compstruct.2012.10.040.

[16] Qi, X. J., Liu, Q. and Shang, F. J. "Dynamic Response of Concrete Arch Bridge under Blast Loading." Applied Mechanics and Materials 501 (January 2014):1283-1286. doi: 10.4028/www.scientific.net/AMM.501-504.1283.

[17] Abbasnia, R. and Nav, F.M. "A Theoretical Method for Calculating the Compressive Arch Capacity of RC Beams Against Progressive Collapse." Structural Concrete 17 (2016): 21-31. doi: 10.1002/suco.201400119.

[18] Farahani, E.M., and Maalek, S. "An Investigation of the Seismic Behavior of a Deck-Type Reinforced Concrete Arch Bridge." Earthquake Engineering and Engineering Vibration 16 (July 2017): 609-625. doi:10.1007/s11803-017-0405-x.

[19] Li, X., Yang, Y., and Pu, Q. "Study on Evaluation and Comparison of the Capability before and after Strengthening of Reinforced Concrete Arch Bridge [J]. " Sichuan Building Science 4 (2007): 98-102.

[20] Nam, J.W., Kim, H.J., Yi, N.H., Kim, I.S., Kim, J.H.J., and Choi, H.J. "Blast Analysis of Concrete Arch Structures for FRP Retrofitting Design." Computers and Concrete 6 (August 2009): 305-318. doi:10.12989/cac.2009.6.4.305.

[21] Hesham, A. N. "Effect of Compressive Strength and Reinforcement Ratio on Strengthened Beam with External Steel Plate." Al-Qadisiya Journal for Engineering Sciences 3 (2010): 148-160.

[22] Gou, H., Pu, Q., Shi, X., and Shi, Z. "Local Stress and Nonlinear Mechanical Behaviors of the V-Shape Pier-Girder Joint Based on Model Test." Advances in Structural Engineering 18 (November 2016): 2193-2205. doi: 10.1260/1369-4332.18.12.2193.

[23] Gou, H., Long, H., Bao, Y., Chen, G., Pu, Q., and Kang, R. "Stress Distributions in Girder-Arch-Pier Connections of Long-Span Continuous Rigid Frame Arch Railway Bridges." Journal of Bridge Engineering 23 (April 2018): 04018039. doi: 10.1061/(ASCE)BE.1943-5592.0001250.

[24] Martinelli, P., Galli, A., Barazzetti, L., Colombo, M., Felicetti, R., Previtali, M., Roncoroni, F., Scola, M., and di Prisco, M. "Bearing Capacity Assessment of a 14th Century Arch Bridge in Lecco (Italy)." International Journal of Architectural Heritage 12(2018): 237-256. doi:10.1080/15583058.2017.1399482.

[25] Augusthus-Nelson, L., Swift, G., Melbourne, C., Smith, C., and Gilbert, M. "Large Scale Physical Modelling of Soil-Filled Masonry Arch Bridges." International Journal of Physical Modelling in Geotechnics 18 (September 2018): 81-94. doi:10.1680/jphmg.16.00037.

[26] Hoehler, M, D McCallen, and C Noble. "The Seismic Response of Concrete Arch Bridges (with Focus on the Bixby Creek Bridge Carmel, California)" (June 1, 1999). doi:10.2172/9869.

[27] Marefat, M.S., Ghahremani-Gargary, E., and Ataei, S. "Load Test of a Plain Concrete Arch Railway Bridge of 20-m Span." Construction and Building Materials 18 (November 2004): 661-667. doi. 10.1016/j.conbuildmat.2004.04.025.

[28] Zhang, J., Li, C., Xu, F., and Yu, X. "Test and Analysis for Ultimate Load-Carrying Capacity of Existing Reinforced Concrete Arch Rib." Journal of Bridge Engineering 12 (January 2007): 4-12. doi:10.1061/(ASCE)1084-0702(2007)12:1(4).

[29] Song, L., Shizhong, Q., and Ying T. "Study on Parameters of Ultimate Bearing Capacity of Reinforced Concrete Arch Bridges." Journal of SouthWest Jiaotong University 3 (2007): 42-47.

[30] Tamura, T., and Murata, H. "Experimental Study on the Ultimate Strength of R/C Curved Beam." Journal of Structural Engineering (May 2010): 1783-1788.

[31] AL-Mutairee, H. M. K. "Effect of Non-Uniform Distribution of Longitudinal Reinforcement on the Behaviour of Reinforced Concrete Horizontally Curved Beams with Fixed-Ends." Journal of Babylon university / Engineering Sciences 21 (2013): 826-838.

[32] Bharadwaj, D., and Purushotham, A. "Numerical Study on Stress Analysis of Curved Beams." International Journal of Mechanical Engineering and Technology 6 (July2015): 21-27.

[33] Muralidharan R., Jeyashree T.M., and Krishnaveni, C. "Analytical Investigation of RC Curved Beams. " Journal of Industrial Pollution Control (October 2017): 1387-1392.

[34] Lee, J.K., and Jeong, S. "Flexural and Torsional Free Vibrations of Horizontally Curved Beams on Pasternak Foundations." Applied Mathematical Modelling 40 (February 2016): 2242-2256. doi:10.1016/j.apm.2015.09.024.

[35] Li, W., Huang, C., and Tang, C. "Negative Angle Vertical Rotating Construction Method of Reinforced Concrete Arch Bridge." Structural Engineering International 27 (March 2017): 558-562. doi:10.2749/222137917X14881937844847.

[36] Chen, B. "Long Span Arch Bridges in China. In Proceedings of Chinese-Croatian Joint Colloquium on Long Span Arch Bridges." Brijuni Islands:[sn] (2008): 119-134. doi: 10.1.1.504.4724.

[37] Kawashima, K., and Mizoguti, A. "Seismic Response of a Reinforced Concrete Arch Bridge." In 12th World Conference on Earthquake Engineering 2000, Paper (No. 1824).

[38] Žderić, Ž., Runjić, A., and Hrelja, G. "Design and Construction of Cetina River Arch Bridge." Proceedings of the 5th International Conference on Arch Bridges (September 2007), Funchal, Madeira, Portugal: 745-750.

[39] Šavor, Z., Mujkanović, N., and Hrelja, G. "Design and Construction of Krka River Arch Bridge." Long Arch Bridges-Proceedings of the Chinese-Croatian Joint Colloquium Long Arch Bridges (July 2008). Fuzhou University, Fuzhou, China: 217-228. doi: 10.1080/15732480600855800.

[40] Franetović, M., Radić, J., and Šavor, Z. "Seismic Assessment of Arch Bridge Across Slunjčica River in Slunj." Conference: 3rd Chinese-Croatian Joint Colloquium on Sustainable Arch Bridges (July 2011), Zagreb, Croatia: 249-258.

[41] Khan, E., Sullivan, T.J., and Kowalsky, M.J. "Direct Displacement–Based Seismic Design of Reinforced Concrete Arch Bridges." Journal of Bridge Engineering 19 (January 2014): 44-58. doi:10.1061/(ASCE)BE.1943-5592.0000493.

[42] Garmendia, L., San-José, J.T., García, D., and Larrinaga, P. "Rehabilitation of Masonry Arches with Compatible Advanced Composite Material." Construction and Building Materials 25 (December 2011): 4374-4385. doi:10.1016/j.conbuildmat.2011.03.065.

[43] Modena, C., Tecchio, G., Pellegrino, C., Da Porto, F., Donà, M., Zampieri, P., and Zanini, M.A. "Reinforced Concrete and Masonry Arch Bridges in Seismic Areas: Typical Deficiencies and Retrofitting Strategies. " Structure and Infrastructure Engineering 11 (2015): 415-442. doi:10.1080/15732479.2014.951859.

[44] Anwar A. M. "Performance of Masonry Arches Strengthened with CFRP Sandwich." Journal of Engineering Sciences Assiut University 43 (November 2015): 823-836.

[45] Valerio A., Giulia M.,Luisa R., Gianfranco S., Mario D., Luciano F., and Raimondo L. " Experimental Investigation on Masonry Arches Strengthened with PRO-FRCM Composite." Composites Part B: Engineering 100 (September 2016): 228-239. doi:10.1016/j.compositesb.2016.05.063.

[46] Iraqi Specification, No. 45/1984, "Aggregate from Natural Sources for Concrete and Construction." (1984).

[47] ASTM C39/C39M-01, "Standard Test Method for Compressive Strength of Cylindrical Test Specimens". Vol. 04.02, 2001. (October 2003): 1-5. doi: 10.1520/C0039_C0039M-16.

[48] ACI (American Concrete Institute), "Code Requirements for Structural Concrete (ACI 318-14) and Commentary." Farmington Hills, MI: American Concrete Institute, 2014.